

# MEASUREMENTS TO DETERMINE POTENTIAL INTERFERENCE TO GPS RECEIVERS FROM ULTRAWIDEBAND TRANSMISSION SYSTEMS

J. Randy Hoffman, Michael G. Cotton, Robert J. Achatz,  
Richard N. Statz, and Roger A. Dalke\*

This report describes laboratory measurements of Global Positioning System (GPS) receiver vulnerability to ultrawideband (UWB) interference. The laboratory measurements were performed by inserting increased levels of UWB interference until an operating GPS receiver lost lock. At each interference level leading up to loss of lock, reacquisition time, fundamental GPS measurements (e.g., pseudorange and carrier phase), status flags (e.g., potential cycle slips), and position data were sampled. A variety of UWB signals were tested, including aggregates of as many as six UWB sources. Two GPS receivers with different receiver architectures were tested.

**Key words:** Global Positioning System (GPS), Ultrawideband (UWB), Impulse Radio, Amplitude Probability Distribution (APD), Interference Measurement, Noise, Radio Frequency Interference (RFI)

## 1. INTRODUCTION

As new wireless applications and technologies continue to develop, conflicts in spectrum use and system incompatibility are inevitable. This report investigates potential interference to Global Positioning System (GPS) receivers by ultrawideband (UWB) signals. According to Part 15 of the Federal Communications Commission (FCC) rules, non-licensed operation of low-power transmitters is allowed if interference to licensed radio systems is negligible. On May 11, 2000, the FCC issued a Notice of Proposed Rulemaking (NPRM) [1] which proposed that UWB devices operate under Part 15 rules. This would exempt UWB systems from licensing and frequency coordination and allow them to operate under a new UWB section of Part 15, based on claims that UWB devices can operate on spectrum already occupied by existing radio services without causing interference. The NPRM calls for further testing and analysis, so that risks of UWB interference are understood and critical radio services, particularly safety services such as GPS, are adequately protected.

Conventional methods of measuring and quantifying interference under narrowband assumptions are insufficient for testing UWB interference. Recently, NTIA's Institute for Telecommunication Sciences (ITS) investigated general characteristics of UWB signals [2]. As a natural extension to the UWB characterization study, this investigation measures the

---

\* The authors are with the Institute for Telecommunication Sciences, National Telecommunications and Information Administration, U.S. Department of Commerce, Boulder, CO 80303.

interference from a representative set of UWB signals imposed on a select group of GPS receivers. The remainder of this section discusses the relevant technologies and associated applications, briefly summarizes related studies, and gives an outline for this report.

## **1.1 The Technologies**

The multifaceted strategic and commercial importance of GPS and the potential commercial importance of UWB are summarized in the following subsections.

### **1.1.1 Global Positioning System**

The Global Positioning System has emerged as a universal cornerstone for much of our technological infrastructure. GPS is a space-based, broadcast-only, radio navigation satellite service that provides universal access to position, velocity, and time information on a continuous worldwide basis. The GPS constellation consists of twenty-four satellites that transmit encrypted high-precision pseudo-random noise (PRN) codes (i.e., P(Y) codes), used by U.S. and allied military forces, and unencrypted coarse-acquisition PRN codes (i.e., C/A codes), which are used in a myriad of commercial and consumer applications.

GPS is a powerful enabling technology that has created new industries and new industrial practices fully dependent upon GPS signal reception. It is presently used in aviation for en-route and non-precision approach landing phases of flight. Precision-approach services, runway incursion, and ground traffic management are currently being developed. On our highways, GPS assists in vehicle guidance, and monitoring; public safety and emergency response; resource management; collision avoidance; and transit command and control. Non-navigation applications are often grouped into geodesy and surveying; mapping, charting, and geographic information systems; geophysical measurement and monitoring; meteorological applications; and timing and frequency. Planned systems, such as Enhanced 911, personal location, and medical tracking devices are soon to be commercially available. Moreover, the U.S. telecommunications and power distribution systems are also dependent upon GPS for network synchronization timing.

### **1.1.2 Ultrawideband Transmission Systems**

Unlike conventional radio systems, UWB devices bypass intermediate frequency (IF) stages, possibly reducing complexity and cost. Additionally, the high cost of frequency allocation for these devices is avoided if they are allowed to operate under Part 15 rules. These potential advantages have been a catalyst for the development of UWB technologies.

UWB signals are characterized by modulation methods that vary pulse timing and position rather than carrier-frequency, amplitude, or phase. Short pulses (on the order of a nanosecond) spread their power across a wide bandwidth and the power density decreases. UWB proponents argue that the power spectral density decreases below the threshold of narrowband receivers, hence, causing negligible interference. Other advantages are mitigation of frequency selective fading induced by multipath or transmission through materials.

Existing and potential applications for UWB technology can be divided into two groups – wireless communications and short-range sensing. In wireless communications, it has been shown to be an effective way to link many users in multipath environments (e.g., distribution of wireless services throughout a home or office). In short-range sensing applications, it can be used for determining structural soundness of bridges, roads, and runways and locating objects and utilities underground. Potential automotive uses include collision avoidance systems, air bag proximity measurement for safe deployment, and fluid level detectors. UWB technology is being developed for new types of imaging systems that would assist rescue personnel in locating persons hidden behind walls, under debris, or under snow.

## **1.2 Brief History of GPS versus UWB Compatibility Measurements**

There are other measurement efforts underway to assess the potential for compatibility between UWB devices and existing GPS receivers. The Department of Transportation (DOT) has sponsored a GPS/UWB compatibility study at Stanford University, focusing on precision-approach aviation receivers that conform to the minimum operational performance standards. The general test procedure was a conducted experiment and utilized a radio frequency interference (RFI) -equivalence concept to relate the impact of UWB signals on GPS to that of Gaussian noise. A second measurement effort at the Applied Research Laboratories of the University of Texas at Austin (ARL/UT) was sponsored by the Ultra-Wideband Consortium. ARL/UT collected fundamental GPS parameters under conducted, radiated, and live-sky conditions for assessing single- and aggregate-source UWB interference to GPS receivers. Data analysis, however, was left to be performed by the GPS and UWB communities.

## **1.3 Scope**

The objective of this study was to measure the degree of interference to various GPS receivers from different UWB signals. Recommendations on UWB regulation are left to the policy teams at NTIA's Office of Spectrum Management (OSM) and the FCC. These measurements were designed to observe and report on broad trends in GPS performance when subjected to UWB interference. No attempt was made to evaluate specific receiver designs or interference mitigation strategies or provide precise degradation criteria.

## 1.4 Organization of this Report

Investigation of UWB interference to GPS receivers encompasses a broad range of expertise including GPS theory and operation, radio frequency (RF) design and hardware implementation, automated measurement development, temporal and spectral characterization of interfering signals, and statistical error analysis. This report completely describes the experiment and is organized as follows.

The first three sections provide orientation and background for the reader. Section 2 describes the characteristics of GPS signals, identifies GPS vulnerability to noise and continuous-wave (CW) interference and describes the nature of UWB signals. Section 3 discusses, at a high level, the general methodologies for measuring GPS performance degradation and describes GPS performance metrics.

Section 4 describes the GPS Interference Test Fixture, experimental procedures, categorization of tested GPS receivers, selected UWB signal parameters, calibration details, signal generation, and power settings. Section 5 describes the methods used for analyzing the collected data. Section 6 displays the experimental results which summarize trends in performance degradation. Conclusions are drawn in Section 7.

Appendices are provided for comprehensive purposes and contain supporting information and detailed measurement results. Appendix A is a comparison between radiated and conducted UWB interference tests. Appendix B describes hardware specifications and settings for the RF components of the test fixture, UWB signal generation equipment, and GPS receivers. Appendix C and D provide measured and theoretical characteristics of all the UWB signal types under test. Appendix E is a brief tutorial on the amplitude probability distribution (APD) which is an important method for characterizing UWB signals. Finally, Appendix F contains a complete set of GPS/UWB interference analysis plots.

## 2. SIGNAL CHARACTERISTICS

The purpose of this section is to describe GPS and UWB signal characteristics in order to identify potential interference scenarios and rationalize measurement procedures.

### 2.1 GPS

GPS is a spread spectrum system. Each GPS satellite is assigned a unique PRN sequence, and all the PRN codes are nearly uncorrelated with respect to each other; therefore, an individual satellite signal is unique and is distinguished through code division multiple access (CDMA). The signals are transmitted at two frequencies: 1575.42 MHz (L1) and 1227.60 MHz (L2). L1 is quadrature-phase modulated with the C/A code and P(Y) code, and L2 is biphasic modulated by the P(Y) code.

Each C/A code has a chipping rate of 1.023 Mchips/s and pseudorandom sequence length of 1023, resulting in a code repetition period of 1 ms. The relatively short periodic nature of the C/A code produces a discrete spectrum with spectral lines spaced 1 kHz apart. Because Gold codes are used to generate the pseudorandom sequences, the spectral envelope deviates slightly from a  $\text{sinc}^2$  shape (common to maximal length codes) with a null-to-null main-lobe bandwidth of 2.046 MHz. Each P(Y) code has a chipping rate of 10.23 Mchips/s and a code repetition period of 7 days. The P(Y) code produces a  $\text{sinc}^2$  power spectral envelope with a null-to-null main-lobe bandwidth of 20.46 MHz and essentially no spectral lines.

Interference imposed on a GPS receiver can have a number of effects. Gaussian-noise interference has the potential to reduce the signal-to-noise ratio (SNR) to such an extent that the GPS receiver can no longer de-correlate the signal. The effects of narrowband interference are more dependent on the proximity to sensitive C/A-code lines in the GPS spectrum. That is, a relatively weak narrowband interfering signal will have little or no effect on the performance of a GPS receiver unless it aligns with a GPS spectral line; if alignment occurs, then interference can be severe.

### 2.2 UWB

UWB signals are difficult to define. One definition of UWB signals describes the spectral emissions as having an instantaneous bandwidth of at least 25% of the center frequency. Other names for UWB, or terms associated with it, include: impulse radio, impulse radar, carrierless emission, time-domain processed signal, and others.

Terminology and definitions aside, the UWB signal is, in general, a sequence of narrow pulses sometimes encoded with digital information. UWB signal pulse widths are on the order of 0.2 to 10 ns and longer. Some have an impulse-like shape and others have many zero crossings. One form of modulation is pulse-position modulation (PPM) where, for example, a pulse that is slightly advanced from its nominal position represents a “zero,” likewise, a slightly retarded pulse represents a “one.” Another form of modulation is on-off keying (OOK) where, for example, an absent pulse represents a “zero.” In addition to the modulation scheme, the pulses can be dithered. In other words, the pulse will be randomly located relative to its nominal, periodic location (absolute dithering) or relative to the previous pulse (relative dithering). For example, 50% absolute dithering describes a situation where the pulse is randomly located in the first half of the period following the nominal pulse location. Finally, some UWB systems employ gating. This is a process whereby the pulse train is turned on for some time and off for the remainder of a gating period.

The frequency domain characteristics (emission spectrum) of a UWB signal are dependent on the time-domain characteristics described above. The pulse width generally determines the overall shape – envelope – of the emission spectrum. The bandwidth of the pulse spectrum generally exceeds the reciprocal of the pulse width. If the pulse train is uniformly spaced, the emission spectrum will have a series of lines. If dithering is used, there will be a smooth component of the emission spectrum in addition to the line component. The higher the dithering, the greater the power contained in the smooth component versus the line component. Some types of modulation can also reduce the spectral line amplitude. Band-limiting changes the characteristics of the UWB signal further.

### **3. GENERAL MEASUREMENT METHODOLOGIES**

In principle, interference testing is straightforward. To wit, an interference test is performed by applying a “foreign” signal to an operating receiver while monitoring receiver performance. Any degradation in receiver performance, beyond what can be expected under normal operating conditions, is then attributed to the interference.

Thus, for our tests, the interfering UWB signal must be fully characterized, GPS receiver operation must be defined in a way that can be measured, and receiver performance must be monitored in a way that is meaningful with respect to its intended application. This section explains these measurement methodologies.

#### **3.1 Interference Characterization**

In real life, UWB and GPS signals are radiated through space and summed within the GPS receiver antenna. In the laboratory, it is easier to control power levels, outside interference, and measurement repeatability if the signals are conducted through cables and added with a power combiner.

However, if conducted signals are used, it is imperative that conducted and radiated signals are characterized and compared to insure that systematic errors are not introduced. Thus, as part of our testing methodology, spectra and waveforms of radiated and conducted UWB signals were measured and compared. The radiated UWB signal was transmitted within an anechoic chamber and received by a GPS receiver antenna while the conducted UWB signal was transmitted through a coaxial cable connected to a power combiner. Results of this comparison, given in Appendix A, show that differences between radiated and conducted UWB signals are negligible.

There are many different types of UWB signals. The one characteristic they all possess, however, is wide bandwidth. Band-limiting by the GPS receiver significantly alters the characteristics of an already diverse signal set. In the past, engineers have found that the amplitude statistics of the interfering signal have the most bearing on whether it will be benign or destructive to the performance of a victim receiver. Thus, as part of our testing methodology, the amplitude of the UWB signals was sampled and statistically analyzed. Two bandwidths were used, corresponding to the bandwidths of two classes of GPS receivers. Results of this test are provided in Appendix C.

### **3.2 Operational Testing**

An operating GPS receiver must be frequency-locked onto the modulated and Doppler shifted carrier frequency, delay-locked onto the C/A code, and phase-locked onto the message. Thus, at a bare minimum, an operating GPS receiver is frequency-, delay-, and phase-locked to a GPS signal.

Two testing methodologies are used to measure the effect UWB interference has on receiver operation or locking. The break lock (BL) operational test determines the BL point defined to be the minimum amount of interference that causes a receiver to lose lock. The reacquisition time (RQT) operational test determines the amount of time it takes a receiver tracking a GPS signal to reacquire the signal after it has been momentarily removed.

The RQT test does not identify an "RQT point" as the BL test identifies a BL point. It is left to others to determine a reasonable RQT and corresponding RQT point for their application. Once this point is established, the BL and RQT operational tests bracket a region of GPS receiver performance degradation. The RQT point sets the lower bound where the interference begins to have a detrimental effect on the operation of the receiver. The BL point sets the upper bound where operation is impossible.

The BL point may differ significantly from receiver to receiver. For example, surveying receivers require flawless carrier phase-lock. General purpose navigation receivers, however, allow imperfect carrier phase-lock but demand stable C/A code delay-lock, and consequently are more tolerant toward some types of interference.

### **3.3 Observational Testing**

An operating GPS receiver calculates user position through the measurement of GPS "observables." Performance degradation of an operating GPS receiver is commonly evaluated through its observables which include pseudorange, carrier phase, Doppler frequency-shift, clock-offset, signal-to-noise ratio, and carrier cycle-slippage. Observables can usually be obtained from the receiver, in real time, through a computer interface.

Various range estimates are computed from these observables, and errors in the range estimates are subsequently statistically analyzed to determine performance degradation. It is not our intent to use results of this analysis to establish precise range-error budgets. Rather, these statistics are intended to support other trends of UWB interference such as RQT degradation. In addition, range error statistics are useful for isolating performance degradation to C/A code delay-locking or carrier phase-locking functions.

## 4. MEASUREMENT SYSTEM AND PROCEDURES

The purpose of this section is to provide a detailed summary of the measurement system, test procedures, GPS-receiver and UWB-signal sample space, signal generation details, and hardware limitations for this experiment.

### 4.1 System

The GPS interference test bed utilized in this experiment was developed at ITS (see Figure 4.1.1). It is comprised of three segments – GPS source, UWB source, and GPS receiver. System configuration is illustrated in Figure 4.1.2 and hardware components are specified in Table 4.1.1 and Appendix B. Each of the contributing signals (i.e., GPS, noise, and UWB) were filtered, amplified, and combined prior to input into the receiver. Signal powers were controlled using precision variable attenuators (VA) controlled by computer. The following subsections provide signal-generation details and justification for hardware employed.

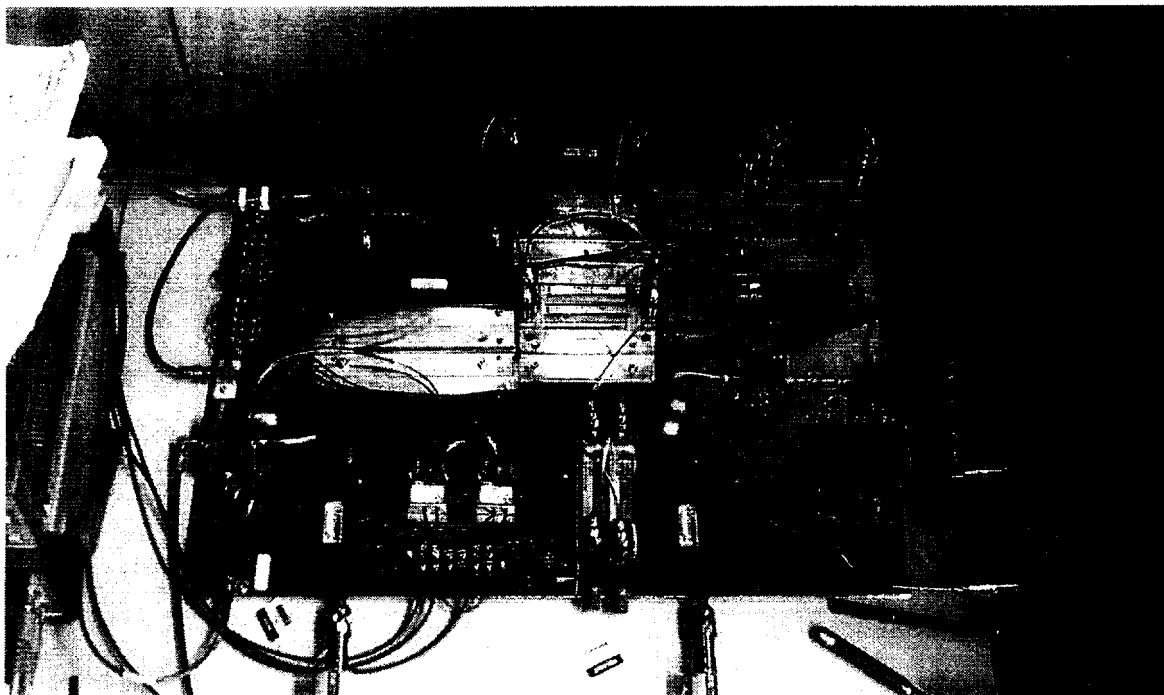


Figure 4.1.1. GPS Interference test bed.

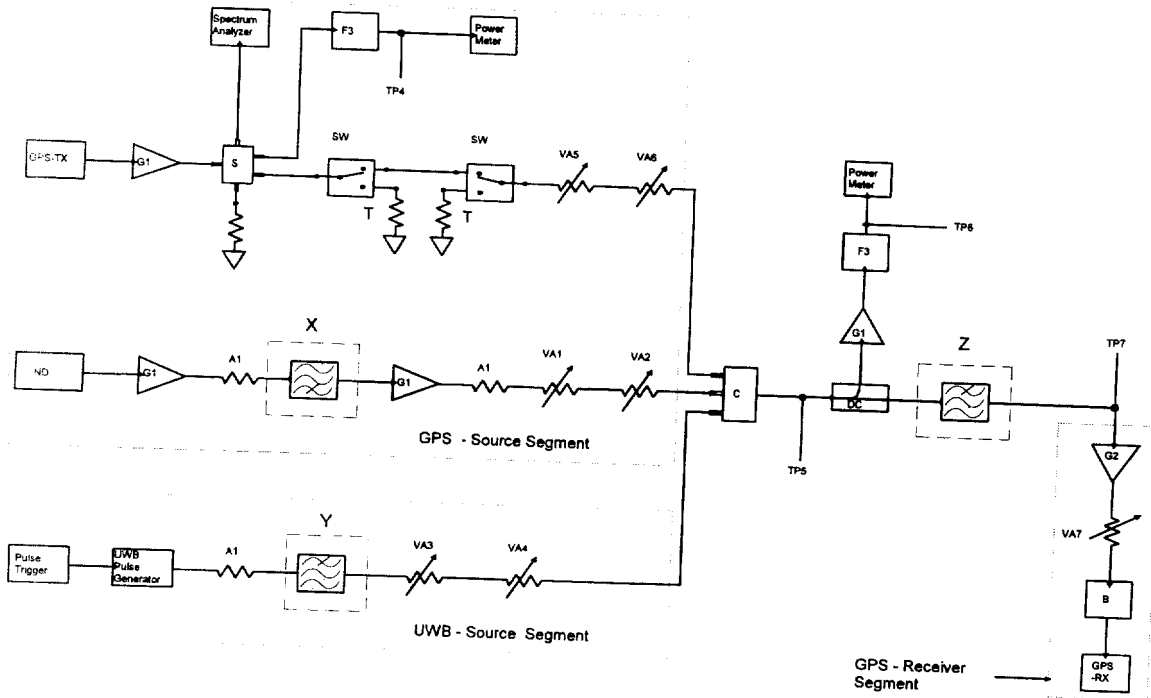


Figure 4.1.2. Block diagram.

Table 4.1.1. Variations in Configuration for Different Receivers

| Receiver Description (Rx #) | Noise Diode | Injected Noise <sup>1</sup> (dBm/20MHz) | Fixture <sup>2</sup> X | Fixture Y | Fixture Z |
|-----------------------------|-------------|---|------------------------|-----------|-----------|
| C/A Code (Rx 1)             | ND1         | -93                                     | F1                     | F1        | Bypassed  |
| Semi-Codeless (Rx 2)        | ND2         | -120                                    | F2                     | F2        | F4/A2     |

<sup>1</sup> Gaussian noise power density (dBm/20 MHz) at point TP7 on the test fixture.

<sup>2</sup> Fixtures X, Y, and Z are shown in Figure 4.1.2, and part number are described in Appendix B

### 4.1.1 GPS-Source Segment

The purpose of the GPS segment is to provide a simulated GPS signal at a known SNR. The GPS signal and background noise were generated with a multi-channel GPS simulator (GPS-TX) and a noise diode (ND), respectively.

Utilization of a GPS simulator provides high-accuracy repetition of scenarios and flexibility for simulation over a wide range of normal and abnormal situations. Generated GPS signals appear as though they had been transmitted from multiple moving satellites, and the simulated satellite positions can be reset to a selected standard configuration at the beginning of each test. Simulated navigation data, required by the user segment and contained in the GPS spread spectrum signal, consists of satellite clock, ephemeris (precise satellite position), and almanac (course satellite position) information.

The GPS simulator used in this experiment is the Nortel model STR2760 provided by the 746<sup>th</sup> Test Squadron at Holloman Air Force Base. It is the responsibility of the 746<sup>th</sup> Test Squadron to verify simulator integrity and consistency by comparing simulated signals to measured data; the STR2760 has met those requirements. It reproduces the environment of a GPS receiver installed on a dynamic platform and accounts for receiver and satellite motion and atmospheric effects (e.g., ionospheric delay, tropospheric attenuation and delay, and multipath).

The receiver location was chosen as 32°N, 106°W, and 1000 m above sea level, and the 75-minute scenario was based on an actual constellation beginning on December 16, 1999 at 9:30 p.m. The simulated signals contain Doppler shifts and variable path lengths through the atmosphere according to satellite motion and elevation angle, respectively. Tropospheric attenuation and multipath were turned off. Also, ionospheric delay was simulated only for the receiver with dual-frequency cross-correlation capability.

In this experiment, we focus on the effects of imposed interference. The minimum number of satellites for a receiver to operate nominally, typically four, was chosen. Satellite geometry during the course of the simulation, shown in Figure 4.1.1.1, produces a Position Dilution-of-Precision (PDOP) between 2 and 3. Space vehicle (SV) 25 was chosen as the focus of the experiment. The transmitted signal powers of the other satellites were set to 5 dB greater than that of SV 25. Therefore, under the same interference conditions the SV-25 SNR will be significantly less than the other satellites, and performance degradation will be isolated to the SV-25 channel. Most importantly, as interference is increased the receiver will lose lock on SV 25 first.

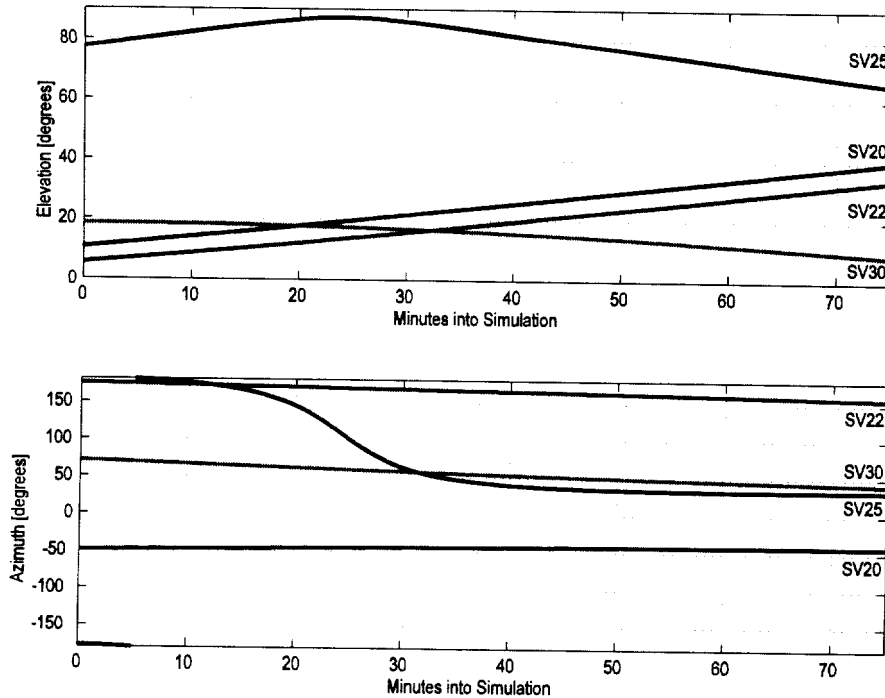


Figure 4.1.1.1. Simulated satellite geometry.

GPS is a CDMA system where multiple transmitters share the same bandwidth. Elevated co-channel interference present with some satellite combinations can produce GPS signal outages. This co-channel interference is approximated with Gaussian noise and emulated with a noise diode in the GPS segment.

#### 4.1.2 UWB-Source Segment

The UWB segment consists of a narrow-pulse generator and a triggering device to create various signals. The pulse shape/width, as a characteristic of the pulse generator, determines the overall spectral envelope. The manner in which the pulses are sequentially spaced (set by the triggering device) determines spectral content within the confines of the envelope. For instance, uniformly spacing the pulses creates strong spectral lines. Dithering the pulse spacing, however, reduces spectral line amplitude and increases noise power density.

The primary criterion for choosing a UWB pulse generator for these measurements depended on whether the spectral envelope was flat and produced sufficient power across the L1 and L2 bands. Two types of UWB pulse generators were utilized, one with a pulse width of 245 ps, and the other with a pulse width of 500 ps. Descriptions of the pulse generators are provided in greater detail in Appendix B. Both pulse generators are triggered by an external device (e.g., arbitrary waveform generator, custom built triggering circuit) to produce different sequential pulse spacings.

For these measurements, the UWB signal is specified by a combination of pulse repetition frequency (PRF), mode of spacing, and the application of gating, all of which have distinctly different effects on spectral and time domain characteristics of the signal.

Four distinct modes of spacing were used: uniform pulse spacing (UPS), on-off keying (OOK), absolute (clock) referenced dithering (ARD), and relative (clock) referenced dithering (RRD). The vertical dashed lines in Figure 4.1.2.1 represent the ticks of a clock. UPS, as the name implies, is a pulse train of equal spacing, where pulses occur at the clock ticks. OOK refers to the process of selectively “turning off” or eliminating pulses at the clock ticks. ARD produces pulses that are dithered in relation to the clock tick. RRD dithers each pulse in relation to the previous pulse position.

The PRF for UPS, OOK, and ARD is equal to the clock rate; for our purposes, the PRF of RRD is defined as the reciprocal of the mean pulse interval. The extent of dither is expressed in terms of the percentage of pulse repetition period, which is the reciprocal of PRF.

Gating refers to the process of distributing pulses in bursts. This is represented in Figure 4.1.2.1 by the removal of the pulses in the shaded areas; in the case of the UPS example, there are 4 pulses generated during the gated-on time followed by 8 clock ticks for which there are no pulses (to give a duty cycle of 33%).

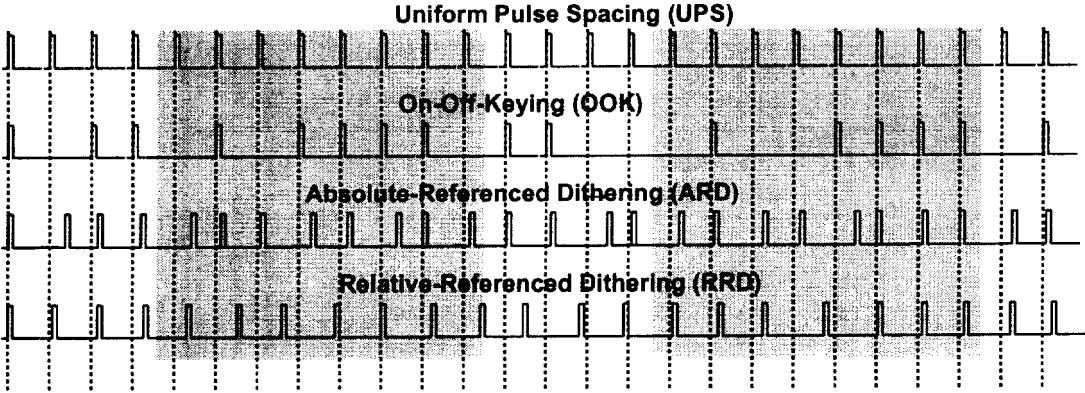


Figure 4.1.2.1. Pulse spacing modes.

### UWB Signal Space

By varying the three parameters – PRF, pulse spacing, and gating – 32 different permutations were chosen to span the full range of existing and potential UWB signals. For these measurements (as shown in Table 4.1.2.1) there are four PRFs (i.e., 0.1, 1, 5, and 20 MHz), four pulse spacing modes (i.e., UPS, OOK, 50% ARD, and 2% RRD), and two

gating scenarios (i.e., no gating and 20% gating with a 4 ms on-time). In addition, various combinations of UWB signals were summed to produce aggregate signals as shown in Table 4.1.2.2.

Table 4.1.2.1. UWB Signal Space

| UWB Signal Parameter       | Range                                       |
|----------------------------|---|
| Average Power Density      | As needed to induce effect on GPS receiver. |
| Pulse Width                | 0.245 and 0.5 nanoseconds                   |
| Pulse Repetition Frequency | 0.1, 1, 5, 20 MHz                           |
| Modulation, Dithering      | UPS, OOK, 50%-ARD, 2%-RRD                   |
| Gating                     | 100% (no gating) and 20% Duty Cycle         |

Table 4.1.2.2. Aggregate UWB Signal Space

| Aggregate | UWB Signal Parameters  |
|-----------|--|
| 1         | 6 × 10-MHz PRF, 2%-RRD, Non-Gated  |
| 2         | 6 × 10-MHz PRF, 2%-RRD, Gated (20% Duty Cycle)   |
| 3         | 2 × 10-MHz PRF, UPS, Non-Gated<br>1 × 3-MHz PRF, UPS, Non-Gated<br>3 × 3-MHz PRF, 2%-RRD, Gated (20% Duty Cycle)   |
| 4         | 3 × 3-MHz PRF, UPS, Gated (20% Duty Cycle)<br>3 × 3-MHz PRF, 2%-RRD, Gated (20% Duty Cycle)  |
| 5         | (a) 1 × 1-MHz PRF, 2%-RRD, Non-Gated<br>(b) 2 × 1-MHz PRF, 2%-RRD, Non-Gated<br>(c) 3 × 1-MHz PRF, 2%-RRD, Non-Gated<br>(d) 4 × 1-MHz PRF, 2%-RRD, Non-Gated<br>(e) 5 × 1-MHz PRF, 2%-RRD, Non-Gated<br>(f) 6 × 1-MHz PRF, 2%-RRD, Non-Gated |

### Spectral Considerations

Spectral plots are shown in Figure 4.1.2.2 for four different UWB signals as they are passed through an L1 bandpass filter. UPS has the power gathered up into spectral lines at intervals of PRF. The greater the PRF, the wider the line spacing, and the greater the power contained in each spectral line. OOK also has spectral lines spaced at intervals of PRF that are superimposed on continuous noise-like spectrum. Dithered signals have spectral

characteristics inherently different from either UPS or OOK. For these measurements, ARD has a pulse spacing that is varied by 50% of the referenced clock period. RRD has a pulse spacing that is varied by 2% of the average pulse period. Both of these dithered cases have spectral features that are characteristic of noise (i.e., no spectral lines).

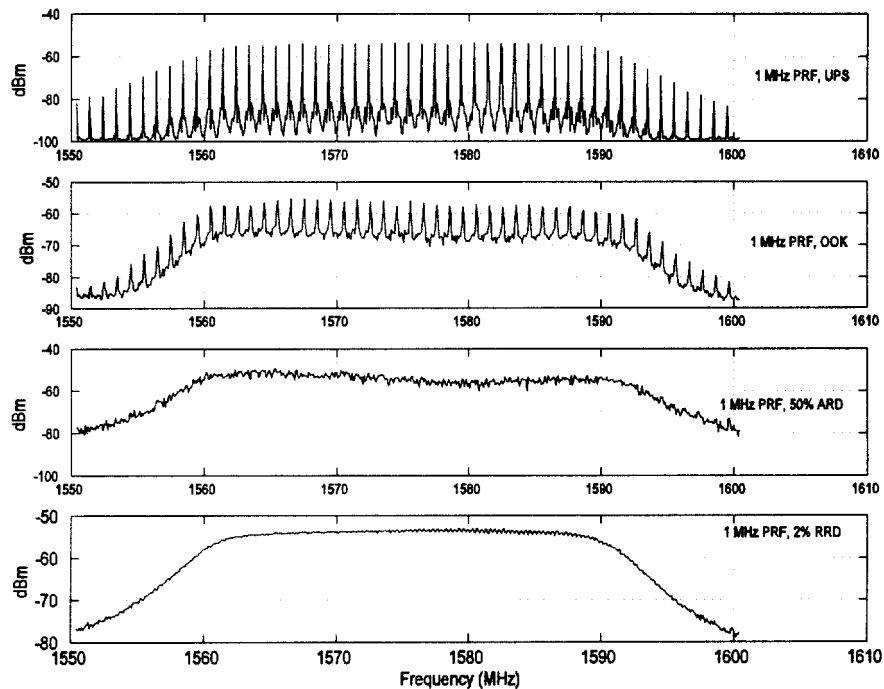


Figure 4.1.2.2. Spectral characteristics of the different pulse spacing modes.

Another feature worth noting is the phenomenon of spectral lines spreading due to gating. The spectrum of the gated UWB signal is the result of convolving the non-gated spectrum with the Fourier transform of the gating signal, which for our purposes is a  $\text{sinc}^2$  envelope. It follows that the single line of the non-gated cases is spread out into a multitude of lines confined by the  $\text{sinc}^2$  envelope, where the spacing between lines, or line spread spacing (LSS), is equal to the reciprocal of the gating period; null spacing, or line spreading null-to-null bandwidth (LSNB), of the main lobe of the  $\text{sinc}^2$  function is equal to two times the reciprocal of gated-on time.

There are two additional spectral features that occur as a result of the signals having been generated by an arbitrary waveform generator (AWG). One is related to how the pattern of pulses is repeated, and the other has to do with the process of placing the pulses into bins, representing discrete dithered pulse spacing. Further discussion of these spectral characteristics of UWB signals is contained in Appendix C.

## Spectral Line Alignment

Because each of the emulated satellites is mobile in nature, there is a corresponding Doppler shift associated with its motion and direction. Figure 4.1.2.3 shows the emulated Doppler frequency for SV 25 going from the beginning to the end of the simulation. Notice that the C/A code lines shift nearly 2.25 kHz over the course of the simulation. For those UWB signals which contain spectral lines, alignment of the UWB spectral lines and the SV-25 spectral lines over a period of 40 minutes is inevitable. To assure controlled measurement conditions, both the GPS simulator and the AWG were time referenced with the same rubidium oscillator and the spectral lines of the UWB signals were precisely placed, as described in detail in Appendix C, Table C.1.1. Figure 4.1.2.4 illustrates the manner in which these spectral lines were placed. Because SV 25 has a particularly vulnerable spectral line at 1575.571000 MHz, each of the UWB signals with discrete spectral lines were created with a spectral line at 1575.570571 MHz – approximately half way between GPS spectral lines. As described in Section 4.3, data acquisition started at 20 minutes into the simulation (at approximately 0 Hz Doppler shift) and continued for the next 20 minutes; hence, spectral alignment was guaranteed.

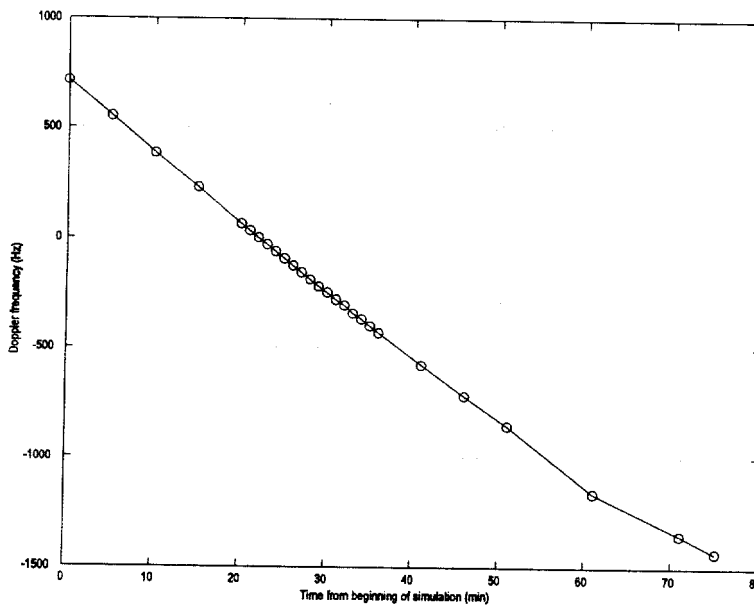


Figure 4.1.2.3. Doppler frequency of SV25.

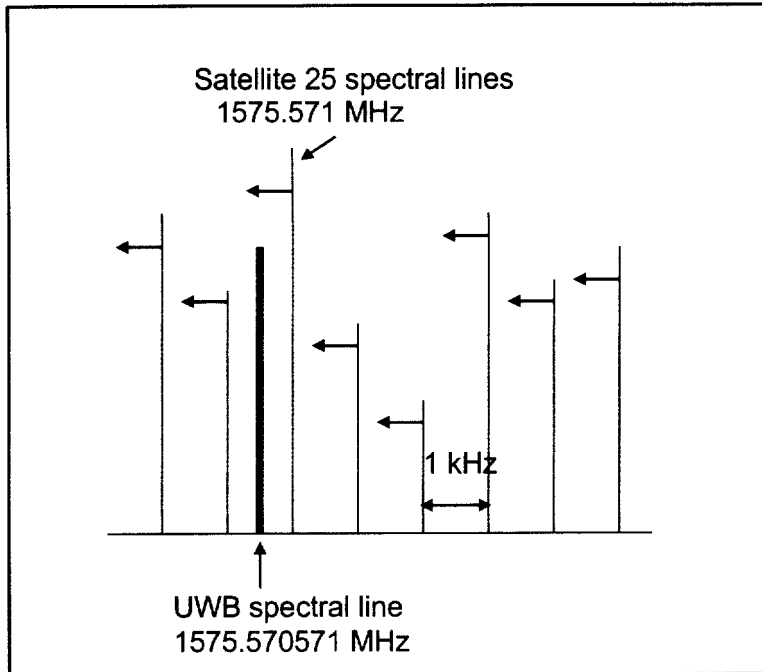


Figure 4.1.2.4. Spectral line placement.

### 4.1.3 GPS-Receiver Segment

The typical stand-alone GPS receiver is implemented on specialized ASICs and DSP chips. The information from GPS signals is processed, according to proprietary adaptive algorithms, to meet design specifications for specific applications. For example, navigational receivers require reliable position information and fast recovery from outages, while surveying receivers require high-precision position accuracy. Each receiver may generate different failure modes from interference and may recover from interference in different ways.

Two receivers encompassing different technologies were selected and are given in Table 4.1.1. These receivers employ various techniques to accomplish their individual design specifications. As a rule of thumb, the receivers under test were left at their factory default settings with two exceptions. First, stand-alone mode was always specified; that is, DGPS, pseudolites, and external sensors (e.g., altimeters, inertial navigation equipment) were disabled. Secondly, carrier smoothing was removed whenever possible in order to minimize the number of correlated data points. Appendix B provides a table of settings for each receiver.

Each receiver has an active antenna with a specific gain and bandwidth. Because the conducted measurements bypassed the antenna, input signals were filtered and amplified to give an equivalent bandwidth and gain of the respective receiver antenna. A preselection filter and low noise amplifier (LNA) were placed in front of the receiver for the purpose of

matching, as close as possible, the filter and amplifier characteristics of the antenna unit. Receiver 2, however, required an active L1/L2 filter with a 27-MHz bandwidth which is approximately half the bandwidth of the accompanying antenna.

It is assumed that the receiver bandwidth sets the narrowest bandwidth for signal path, and therefore, the equivalent antenna bandwidth filter is not critical to the outcome of the results. This was verified by measurements using two different equivalent antenna bandwidths for the same receiver. However, for practical purposes, the preselector filters were also used to prevent saturation of amplifiers utilized in the test fixture. The discussion on radiated versus conducted measurements, given in Appendix A, is also relevant to this topic.

## 4.2 Power Measures, Settings, and Calibration

The purpose of this section is to clarify power measurement terminology, discuss power level settings of the various signal sources, and describe the calibration procedures used to assure the proper power levels.

### 4.2.1 Carrier-to-Noise Density Ratio Settings

To account for other potential sources of interference, such as sky noise, cross-correlation noise from other satellites within the GPS constellation, and GPS augmentation systems, broadband noise was added to the GPS-source segment. The level of broadband noise – based on minimum  $C/N_0$  requirement for acquisition of a GPS satellite – was set to 34 dB-Hz [3]. Based on the minimum guaranteed GPS signal power ( $C$ ) specification for the C/A code of -130 dBm into a 0 dBic gain antenna [4] and a 2 dB implementation loss ( $L_{imp}$ )<sup>1</sup> the maximum broadband noise density level at which satellite acquisition can be ensured is:

$$N_0 = C - L_{imp} - C/N_0 = -130 - 2 - 34 = -166 \text{ dBm/Hz.}$$

Because the broadband noise was measured at the output of a 20-MHz bandpass filter, the added-noise power level is then calculated as:

$$N = -166 + 10 \log (20 \times 10^6) = -93 \text{ dBm/20 MHz.}$$

The use of a broadband noise level based upon the  $C/N_0$  acquisition threshold is supported by computer simulations performed within the International Telecommunication Union Radiocommunications Sector (ITU-R). The simulations in ITU-R Recommendation M.1477 show how  $C/N_0$  can vary over a 24-hour period, at different user locations, when only sky

---

<sup>1</sup> The implementation loss takes into account the loss due to IF filtering, the loss due to the analog-to-digital conversion, correlation loss due to modulation imperfections in the GPS signal and other miscellaneous losses.

noise and GPS cross-correlation noise are considered. The results of this simulation indicate that without any additional interference from external sources, and under certain worst case conditions, the  $C/N_0$  level can fluctuate to within 1 dB of the acquisition threshold of 34 dB-Hz.

#### 4.2.2 Calibration and Power Level Correction

For these measurements, all signal powers were measured with a power meter and expressed as a mean value. Wideband sources, such as UWB signals and noise, are expressed in terms of power density in a 20-MHz bandwidth (centered at 1575.42 MHz). This section describes the various steps taken to assure power-level accuracy.

To assure that no test-fixture amplifier became saturated throughout the measurements and verify functionality, power levels were measured throughout the test fixture using the full range of signals and power levels. Amplifiers, in addition, were tested for linearity – also using the full range of signals and power levels.

Prior to every interference measurement, power levels of the GPS, noise, and UWB signals were measured without attenuation imposed. Measured power at TP4 and TP6 (in Figure 4.1.2) are referenced to the input of the LNA (TP7) via calibration factors which account for the losses associated with individual power-measurement paths. During the test, contributing power levels were determined by subtracting an applied attenuation from the respective 0-dB attenuation measurements. Additionally, each attenuator was checked for integrity before each test.

Because noise was measured in a bandpass filter centered at the L1 frequency, and because some power passed through the filter outside the 20-MHz bandwidth, a power correction was applied. This correction factor was determined by passing the noise through the filter and measuring the noise power with a spectrum analyzer over a range of frequencies centered at 1575.42 MHz. The power was integrated over 100 MHz and then integrated again across 20 MHz. The difference between these two values (in dB) is subtracted from the measured noise power, giving a spectral power density in the 20 MHz bandwidth.

To assure proper and consistent power levels at the output of the GPS simulator, the GPS signal power of SV 25 was measured at the beginning of each test. All other satellites were turned off during power measurement. To reduce the noise contribution and exclude the L2 signal, the power was measured through an L1 bandpass filter centered at 1575.42 MHz; however, because the power meter measures both the C/A and P code, a calibration factor was applied to determine the power of the C/A code only. This calibration factor was determined by measuring and theoretically verifying the difference in power levels between having only the C/A code turned on and having both the P and C/A codes turned on.

Two other issues regarding power settings has to do with measuring and setting the power of gated and aggregate signals. Because the power meter does not accurately measure gated signal powers, all gated signal powers were measured without gating. As mentioned earlier, the power of all gated signals, used during interference measurements, is expressed as the average power of the non-gated signal. Twenty percent gating reduces mean non-gated signal power by 7 dB. Finally, all signals contributing to the aggregate signals shown in Table 4.1.2.2 have equal peak powers.

### 4.3 Measurement Procedure

In this experiment, two separate tests were performed to measure break-lock and reacquisition-time behavior (flowcharts are given in Figures 4.3.1 and 4.3.2, respectively). The procedures were implemented in software to enhance repeatability, automate testing, and provide a vehicle for extracting information from the receivers.

During RQT measurements, the GPS simulator used a dynamic scenario emulating a mobile receiver traveling at 10 m/s. During BL measurements, a static scenario was used. The measurements were delayed 20 minutes every time the simulator was reset. This twenty-minute delay is based on the fact that it takes a minimum of 12.5 minutes for the receiver to download the entire navigation message from the constellation; hence, we assume 20 minutes is enough time for the almanac/ephemeris data inside the receiver to be up-to-date and complete.

The basic BL measurement consists of turning off interference, reestablishing lock, turning on interference, and sampling the receiver's loss-of-lock indicator once per second over the BL measurement duration (approximately 17 minutes). The BL test shown in Figure 4.3.1 determines the BL point. This is accomplished by incrementing UWB signal power by 3 dB between BL measurements until BL occurs. The BL test then decrements the UWB signal power in 1-dB steps until lock is maintained continuously over the entire measurement duration. The BL point is defined as 1 dB above this final UWB signal power. During BL measurements, the following observational parameters were sampled once per second for data analysis: pseudorange, observation time, clock offset, carrier phase, Doppler frequency shift, signal-to-noise ratio, potential cycle slip, position data, and receiver tracking status.

The basic RQT measurement consists of turning off the zenith satellite, setting the interference level, delaying 10 seconds, turning on the zenith satellite, applying the interference, and measuring the number of seconds until the receiver achieves lock. A RQT measurement is successful if lock is achieved within 2 minutes and maintained for at least 1 minute. The RQT test summarized by the flowchart in Figure 4.3.2 is performed by incrementing UWB signal power by 3 dB between sets of 10 RQT measurements. The test is complete when all 10 RQT measurements at a single UWB power are unsuccessful.

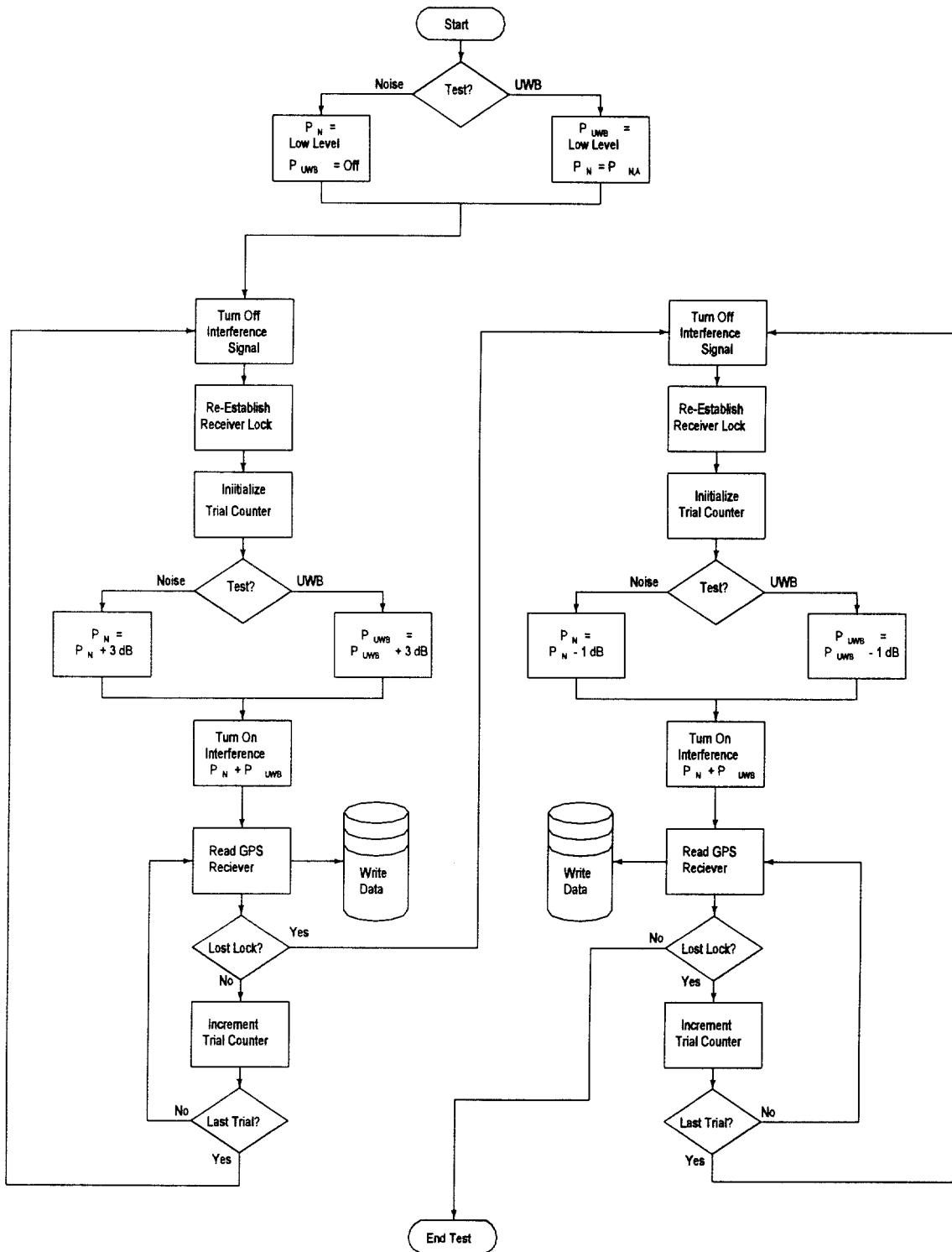


Figure 4.3.1. Break-lock test flowchart.

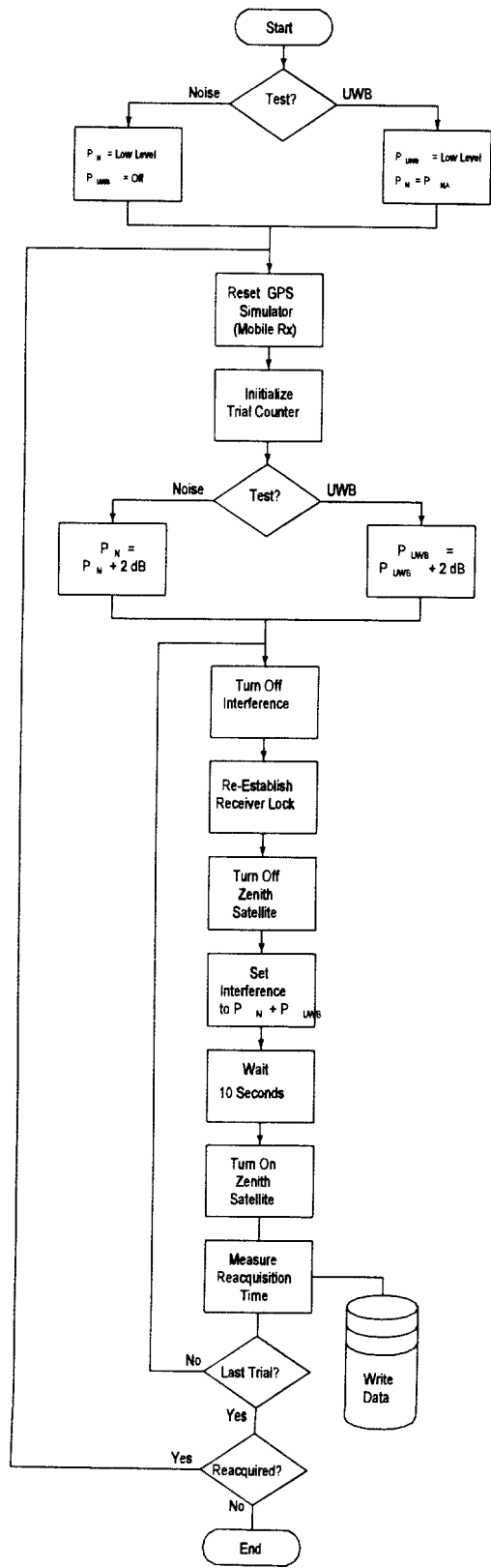


Figure 4.3.2. RQT test flowchart.

## 5. DATA ANALYSIS

Data analysis consists of characterizing the UWB interference and quantifying the effects of the interference on GPS receiver signal acquisition, signal tracking, and range estimation functions. The effects of UWB interference on signal acquisition and signal tracking are characterized with the BL point and RQT operational metrics. The effects of UWB interference on range estimation are characterized with observational metrics such as the statistics of range error.

### 5.1 UWB Signal Characterization

Band-limited UWB signals can be decomposed into time-varying amplitude and phase functions. Engineers, in the past, have found strong correlation between signal amplitude statistical characteristics and receiver performance. Therefore it should not be surprising that signal amplitude statistical characteristics are suspected as being correlated to GPS receiver performance degradation.

Signal amplitude statistics are often visualized with the APD. The APD shows the probability or percent of time a signal will exceed an amplitude value. Formally:

$$F_A(a) = P(A > a) \text{ ,}$$

where  $A$  is the amplitude random variable and  $a$  is an amplitude value. The APD is the compliment of the amplitude cumulative distribution function (CDF) which describes the probability a signal amplitude will be less than or equal to an amplitude value. The APD can also be written in terms of the CDF as:

$$F_A(a) = 1 - P(A \leq a) \text{ .}$$

APDs are often plotted on a Rayleigh graph where the amplitude of Gaussian noise is represented by a negatively sloped, straight line. Gaussian noise mean power corresponds to the power at the 37th percentile.

Non-Gaussian signals have APDs that deviate from the straight line when plotted on a Rayleigh graph. Non-Gaussian signal mean power cannot be read directly from the APD. However, when the power samples are normalized by some reference power, power ratios (peak-to-mean or peak-to-median) can be determined. In addition, the percentage of time a non-Gaussian signal is present can be read from the APD.

The “Gaussian-ness” of the band-limited UWB signal is dependent on the signal pulse repetition frequency and pulse-spacing specifications and the bandwidth of the receiver filter. Figure 5.1.1 shows two UWB signal APDs along with a Gaussian noise APD. The curves are normalized to 0-dBm/20MHz mean power. The first APD corresponds to a UWB signal with a 1-MHz PRF and uniform pulse spacing. The second APD corresponds to a UWB signal with a 1-MHz PRF and 2% relative referenced dithering. Because the PRF is much less than the bandwidth, the pulses are resolved, and the amplitude statistics are nearly identical. Therefore, the two curves lie on top of each other. Both have approximately 10 dB peak to mean power ratios. The pulse is present approximately 60% of the time.

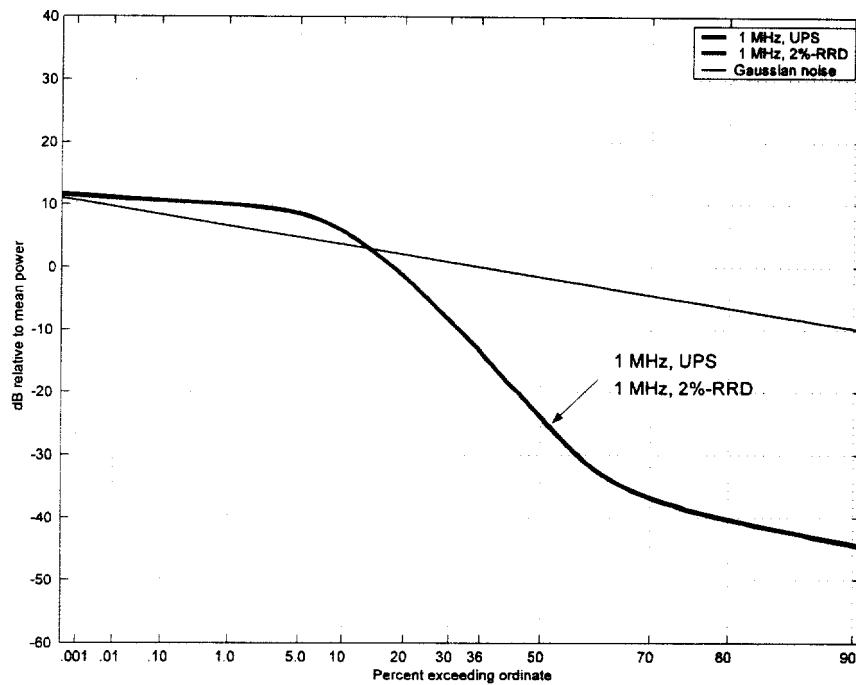


Figure 5.1.1 APDs for Gaussian noise, 1-MHz PRF with UPS, and 1-MHz PRF with 2% RRD.

A complete collection of APDs derived from samples of UWB interferers used during BL and RQT tests can be found in Appendix C. These APDs were acquired with 3 MHz and 20 MHz bandwidths. A detailed tutorial on the APD can be found in Appendix E.

## 5.2 Operational Metrics

### 5.2.1 Break-lock Point

The BL point is the UWB signal power level that causes a receiver in tracking mode to re-enter acquisition mode. For some receivers, BL refers to the failure of C/A code delay tracking while for other receivers, BL refers to loss of carrier phase tracking.

Theoretically BL is a binomially distributed random process - the receiver is either locked or not. Thus BL can occur over a range of UWB signal levels and is likely to vary with BL measurement duration. Rather than assigning a BL point, it would be more accurate to assign a BL probability to every UWB signal level tested. Unfortunately, repeated BL measurements at various power levels and BL measurement durations are not practical.

Thus, for analysis purposes, the BL point is defined to be 1 dB above the maximum UWB signal power, where the receiver is able to maintain lock during the entire BL measurement duration, while the BL test is decrementing. At times, the receiver was able to maintain lock at a UWB signal power when the BL test was incrementing but lost lock at the same level while the BL test was decrementing. In this case the BL point is defined to be 1 dB above this UWB signal power.

### 5.2.2 Reacquisition Time

The RQT is the time it takes a receiver, forced from tracking to acquisition by the sudden removal of the satellite signal, to reenter tracking mode. As in BL, for some receivers tracking refers to the C/A code delay tracking, while for other receivers it refers to the carrier phase tracking.

RQT is assumed to be a Gaussian distributed random variable. However; no test was formally conducted to confirm this. Furthermore, there is a binomially distributed element to the RQT test since RQT measurements are not always successful. A RQT measurement is unsuccessful when reacquisition is not obtained in less than  $RQT_{max}$  seconds. When the measurement is unsuccessful, in principle, no RQT exists.

Rather than ignore the unsuccessful measurement a new random variable was defined:

$$\kappa = \min(RQT, RQT_{max}) .$$

The mean  $\kappa$  was then used for analysis purposes:

$$m_{\kappa} = \frac{1}{N} \sum_{n=1}^N \kappa_n ,$$

where  $N$  is the number of RQT measurements.

If all measurements are successful, then mean  $\kappa$  is equivalent to the mean RQT. This is no longer true if at least one measurement is unsuccessful. The advantage of using mean  $\kappa$  is that it steadily converges to  $RQT_{\max}$  with increasing UWB signal level. In contrast, mean RQT becomes more variable due to the decrease in the number of successful measurements.

### 5.3 Observational Metrics

Range, cycle slip, and SNR observational metrics were derived from data acquired during the BL measurement. Cycle slip and SNR require minimal additional processing. However, range requires a considerable amount of processing to yield useful analysis information.

#### 5.3.1 Range Performance

Degradation of the range estimate is determined by analysis of range error statistics. Range error values were derived from subtracting a known, simulated range from the range measured by the GPS receiver. The range error statistic was found to be time dependant and therefore non-stationary. This non-stationarity was introduced by systematic errors due to the GPS radio environment and spectral line interference. A calibration and correction procedure was developed to remove the systematic component, giving a range error residual – the statistics of which were then used for analysis.

#### Range

Two range estimates – pseudorange (PSR) and accumulated delta-range (ADR) – were derived from observables sampled during the BL measurement. PSR is the most fundamental range measurement derived from correlation of the C/A code. The prefix *pseudo* highlights the fact that satellite and receiver clocks are not synchronized. ADR is an ambiguous range corresponding to the accumulated differences in range from one time to another. ADR is derived from observation of the Doppler-shifted radio frequency carrier. Although the ADR is ambiguous, it has much less uncertainty than PSR. This ambiguity can be resolved with a time-averaged code-minus-carrier (CMC) range bias which is defined to be the difference between the PSR and ADR.